CHEMISTRY
A EUROPEAN JOURNAL

DOI: 10.1002/chem.201002605

Antisymbiotic Self-Assembly and Dynamic Behavior of Metallamacrocycles with Allylic Corners

Inmaculada Angurell,[a] Montserrat Ferrer,*[a] Albert Gutiérrez,[a] Manuel Martínez,[a] Laura Rodríguez,[a] Oriol Rossell,[a] and Marianne Engeser[b]

The design and synthesis of discrete supramolecular architectures by metal–ligand self-assembly is an area of current interest.[1–11] The application of the directional bonding approach has proved to be very versatile, allowing the synthesis of many molecular triangles, squares, rectangles, pentagons, hexagons, and cages.[12–18] Among them, homometallic molecular squares, formed by the reaction of *cis*-protected square planar complexes with linear symmetric ditopic ligands, have been the most widely studied.[19–25] The assembly of metallamacrocycles containing different metal corners and/or nonsymmetric ligands using this method presents additional difficulties due to the possible generation of a mixture of isomers that are difficult to separate. To overcome this, they are generally obtained through modular self-assembly methodology. This strategy requires the initial synthesis of mononuclear complexes with strong covalently bound ligands that have additional donor sites available for coordination to further acceptor building blocks.[26–28] Nevertheless, several molecular triangles and squares have been recently assembled following the directional bonding approach by using nonsymmetric linkers and identical metal corners. Interestingly, in some cases, unexpected self-selection of a single linkage isomer was observed.[29–33] To analyze the large quantity of metallamacrocycles reported to date, the following classification is proposed, according to the nature of the assembled units: 1) species containing identical metal corners and symmetric linkers; 2) species containing identical metal corners and nonsymmetric linkers; and 3) species containing different metal corners and nonsymmetric linkers.

Herein, we report the use for the first time of the directional bonding approach for the synthesis of metallamacrocycles displaying two different metal corners connected by a nonsymmetric ditopic linker. By the correct choice of the different units, that is, metal corners and ambidentate ligand, we have been able to promote its self-assembly producing molecular square architectures and, more interestingly, achieving the self-selection of a single linkage isomer.

Evidently, the correct choice of a heteroditopic ligand in which the different (stereo)electronic characteristics of the donor groups could control the reactivity at the metal site is decisive. Thus, we focused our attention on the 4-PPh_2py ligand (py = pyridine), given its hard-soft character.[34,35]

Furthermore, the electronic nature of the ancillary ligands in the metal corners on the proposed assembly is also crucial for the self-selection process. As a result, complex [Pd(η^3-2-Me-C_3H_4)(cod)](CF_3SO_3) was chosen as the source of {Pd(η^3-2-Me-C_3H_4)}$^+$, a potential metal corner that could provide a varied reactivity to the system, as expected for the allyl palladium species. On the other hand, the complex [Pd(H_2O)$_2$(dppp)](CF_3SO_3)$_2$ was chosen as the second metal corner supplier, {Pd(dppp)}$^{2+}$ (dppp = bis(diphenylphosphino)propane). The selected metal fragments were expected to coordinate selectively to each of the donor atoms of the heteroditopic 4-PPh_2py ligand. Following Pearson's antisymbiotic effect,[36] the greatest stability is expected when the softest ligands are bonded *trans* to the hardest ones.

With these three components in our hands, that is, [Pd(η^3-2-Me-C_3H_4)(cod)](CF_3SO_3), [Pd(H_2O)$_2$(dppp)](CF_3SO_3)$_2$, and 4-PPh_2py, the self-assembly was explored in solution in dichloromethane at room temperature (Scheme 1). After several minutes, the color of the solution faded away and the ^{31}P NMR spectrum (Supporting Information, Figure S1) showed two signals associated with the P atoms of the dppp ligand and those bonded to the allylpalladium fragment, respectively, indicating the presence of only one species in solution. This species, the targeted macrocycle **1**, was obtained

[a] Dr. I. Angurell, Dr. M. Ferrer, Dr. A. Gutiérrez, Prof. M. Martínez, Dr. L. Rodríguez, Prof. O. Rossell
Departament de Quimica Inorgànica, Universitat de Barcelona
Martí i Franquès 1-11, 08028 Barcelona (Spain)
Fax: (+34)934907725
E-mail: montse.ferrer@qi.ub.es

[b] Dr. M. Engeser
Kekulé-Institut für Organische Chemie und Biochemie
der Universität, Gerhard-Domagk-Str.1, 53121 Bonn (Germany)

Supporting information for this article is available on the WWW under http://dx.doi.org/10.1002/chem.201002605.

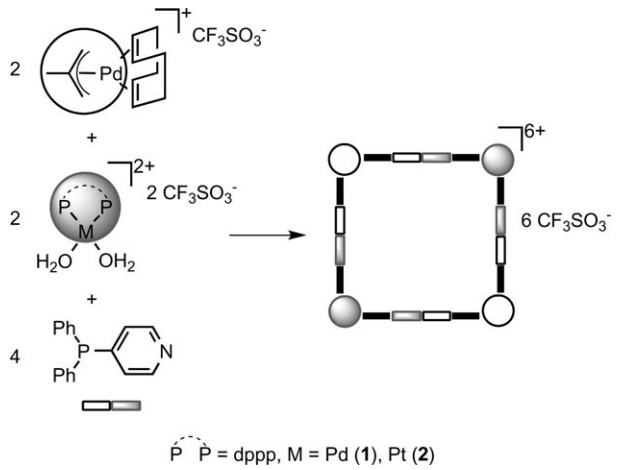

Scheme 1. Self-assembly of metallamacrocycles **1** and **2**.

as a yellow solid after precipitation with diethyl ether in 85% yield. The ^{1}H NMR spectrum of **1** in $CDCl_3$ (Figure 1, top) shows chemically nonequivalent resonances for both α and β proton pairs of the pyridyl rings, as a result of the hindered rotation about the Pd–N bond. Similarly, those of the CH_2 of the dppp ligand are nonequivalent due to the lack of a molecular mirror plane; the signals due to allyl groups (methyl, *syn*- and *anti*- protons) were also present. The comprehensive assignment for all of the resonances has been carried out by using COSY ^{1}H–^{1}H (Supporting Information, Figure S2), HSQC ^{1}H–^{13}C, and ^{1}H{^{31}P} NMR spectroscopy experiments. The formation of **1** is further supported by ESI-FT-ICR mass spectrometry (Supporting Information, Figure S3).

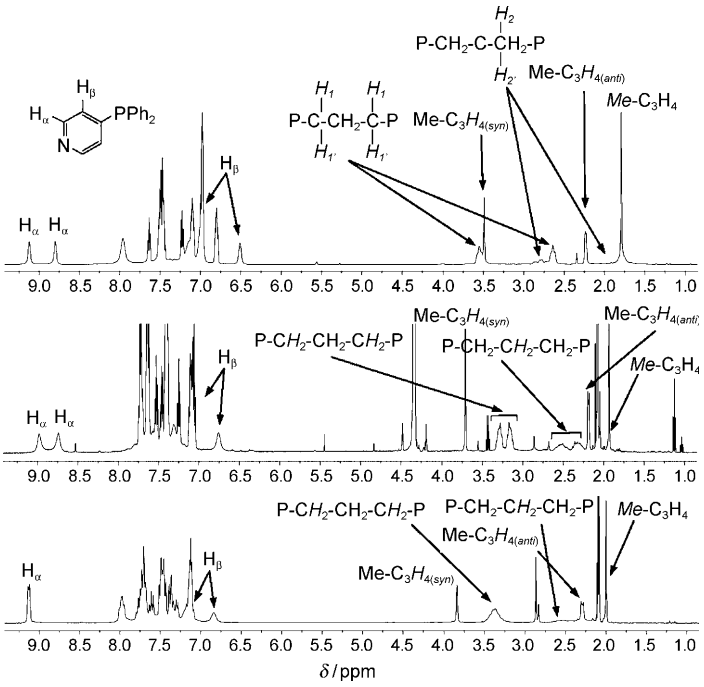

Figure 1. ^{1}H NMR spectra of complex **1** at 298 K; top: $CDCl_3$, middle: [D_3]nitromethane, and bottom: [D_6]acetone.

By using the same methodology, the self-assembly of $[Pd(\eta^3\text{-}2\text{-}Me\text{-}C_3H_4)(cod)](CF_3SO_3)$, $[Pt(H_2O)_2(dppp)](CF_3SO_3)_2$, and 4-$PPh_2$py produced the analogous Pd_2Pt_2 macrocycle **2** (Scheme 1). Spectroscopic data (see S4–S6 in the Supporting Information) agreed with the expected nature of the heterometallamacrocycle. Furthermore, its complete characterization has been achieved from the X-ray crystal structure determination of a single crystal formed by slow diffusion of hexane into a solution of **2** in dichloromethane.[37] The unit cell shows three independent but closely similar metallacycles, as well as the corresponding triflate anions and crystallization solvent molecules. As featured in Figure 2, the crystal structure shows a macrocyclic assembly

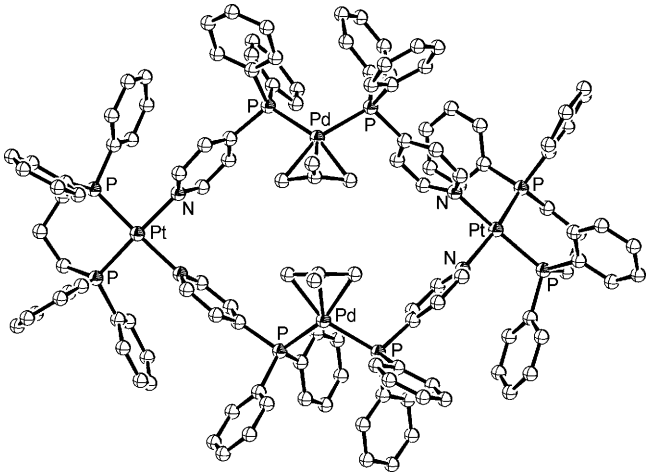

Figure 2. ORTEP plot (50% elipsoids) of one of the cationic units of **2**.

containing alternating palladium and platinum atoms situated at the corners of a cationic tetranuclear unit; the structure can be described as having a butterfly shape with an idealized C_{2h} symmetry. The distance between the platinum (ca. 13 Å) and the closer palladium centers (ca. 6 Å) in each metallamacrocycle represents a measure of its cavity. Each edge is spanned by a 4-PPh_2py ligand with Pd–P and Pt–N average distances being 2.31 and 2.11 Å, respectively, both in the range reported for these bonds. The distorted square planar configuration around the palladium atoms is achieved by the coordination of one allyl ligand in an η^3-fashion and two phosphorus atoms of the 4-PPh_2py ligands. Each platinum(II) center also shows a distorted square planar environment with the coordination of two nitrogen atoms of the ditopic 4-PPh_2py, plus two phosphorus of the chelating dppp ligand. The cationic macrocycles are stacked in an almost eclipsed fashion forming one-dimensional columns along the *a* axis of the crystal (Figure 3) and include some of the triflate anions. The Pd···Pd and Pt···Pt distances between the stacked cycles in the solid state are approximately 14 Å. Short contacts (ranging from 2.99–3.05 Å) between triflate oxygen atoms and pyridine carbons (Supporting Information, Figure S7) are found in a similar way to that reported for other systems.[38–40]

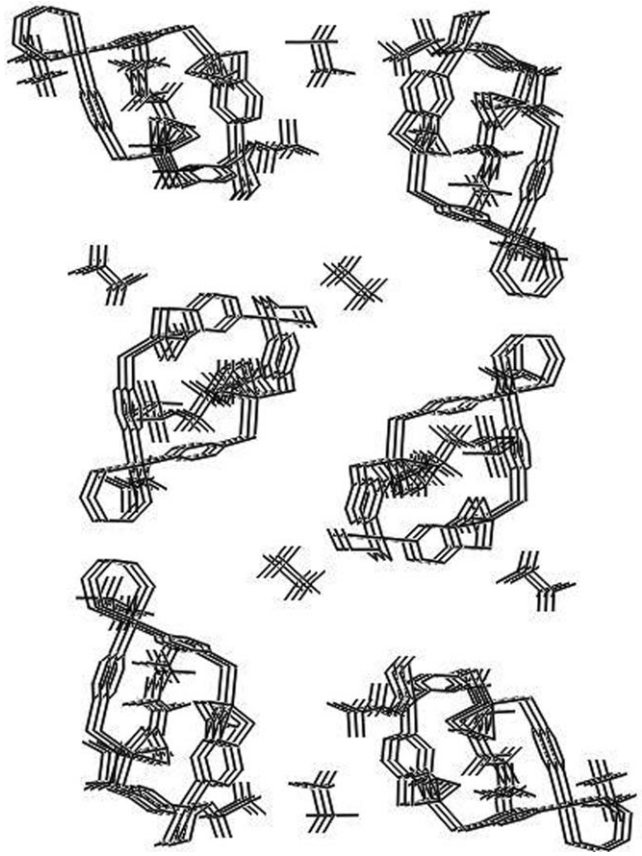

Figure 3. Packing diagram of **2** viewed parallel to the *a* axis. The figure shows the columns formed by the superposition of macrocycles together with the location of the triflates. Phenyl groups are omitted for clarity.

It is interesting to note that the ^{1}H NMR spectra of the macrocycles **1** and **2** are solvent- and temperature-dependent. As indicated above, the ^{1}H NMR spectra of both **1** and **2** in $CDCl_3$ at room temperature revealed two sets of signals for both H_α and H_β proton pairs of the pyridine rings, and four different peaks corresponding to the protons of the aliphatic chain in dppp. However, in the more coordinating [D_6]acetone solvent (Figure 1, bottom), only the splitting of the H_β proton pair is detected and two broad peaks for the dppp protons appear. Furthermore, the spectrum in [D_3]nitromethane at room temperature (Figure 1, middle) shows an intermediate situation, in which the two H_α proton signals, and the broad signals attributed to the protons of the dppp are close to coalescence. Effectively, temperature-dependent ^{1}H NMR spectroscopy of **1** in [D_3]nitromethane (Supporting Information, Figure S8) indicates that the resonances of H_α and H_β proton pairs coalesce at about 310 and 330 K respectively. A NOESY NMR spectroscopy experiment in $CDCl_3$ (Supporting Information, Figure S9) showed the expected H_α–$H_{\alpha'}$ and H_β–$H_{\beta'}$, H_1–$H_{1'}$ and H_2–$H_{2'}$ correlations, as well as the expected H_{anti}–H_{syn} of the allyl group. With the NMR spectroscopy data available it was not possible at this point to postulate unambiguously a mechanism that could explain the dynamic behavior of these supramolecular structures. However, the fact that the dynamic behavior is solvent dependent suggested that the process involves more than a simple pyridine rotation.

In view of the results reported in the literature on the existence of both spontaneous and ion-paired hindered rotation of pyridine rings in other related systems,[41–43] the kinetico-mechanistic study of the observed nonrigidity for compound **1** was further pursued. The gross mobility of the α and β protons of the pyridine rings has been studied in $CDCl_3$ solution by magnetization transfer experiments, as well as full line-shape analyses.[44–46] Figures 4 and 5 collect some of the results obtained for these experiments.

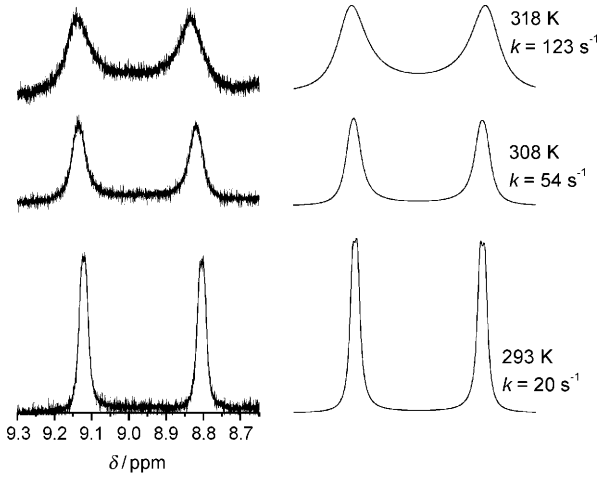

Figure 4. 1H NMR ($CDCl_3$, 500 MHz) spectral data of **1** used for the full line-shape analysis of the exchanging resonances of H_α and H_β pairs.

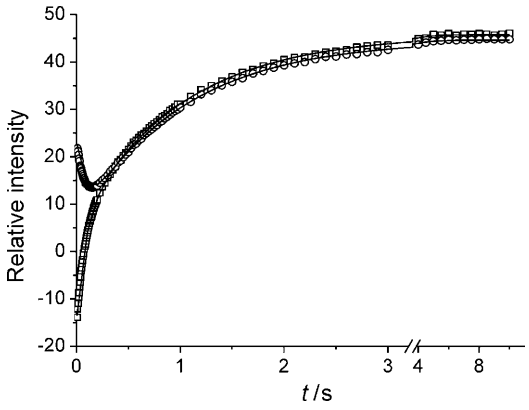

Figure 5. Experimental points and fitted curve for the magnetization transfer experiment on compound **1**. □ = recovery of the inverted signal at $\delta = 9.10$ ppm, ○ = inversion/recovery of the signal at $\delta = 8.80$ ppm.

The results derived from the two sets of experiments are in excellent agreement and a joint Eyring plot can be generated (Supporting Information, Figure S10) producing $\Delta H^{\neq} = (46 \pm 3)\ \mathrm{kJ\,mol^{-1}}$ and $\Delta S^{\neq} = (-61 \pm 10)\ \mathrm{J\,K^{-1}\,mol^{-1}}$ as the thermal activation parameters for the spontaneous ex-

change. Thus, it is clear that a single rate determining step is observed for the mentioned gross process. The values obtained for the apparent thermal activation parameters are within the range of those obtained for processes on the systems indicated above.[41–43] Further studies have been carried out in the presence of added tetrabutylammonium triflate in 1:40 and 1:60 ratios (macrocycle/triflate added), and the results indicated an important increase in the rate of the mobility on increasing the ionic strength of the solution (Supporting Information, Table S1). Moreover, an important aspect is the decrease of the values of the thermal activation parameters on increasing the concentration of triflate in the reaction medium ($\Delta H^{\neq} = (30 \pm 4)\ kJ\,mol^{-1}$ and $\Delta S^{\neq} = (-110 \pm 15)\ J\,K^{-1}\,mol^{-1}$, and $\Delta H^{\neq} = (26 \pm 1)\ kJ\,mol^{-1}$ and $\Delta S^{\neq} = (-125 \pm 4)\ J\,K^{-1}\,mol^{-1}$, for a 1:40 and 1:60 ratio respectively). These data are a clear indication of an associative activation process[47] being favored in the presence of significant amounts of anionic counterparts. It is important to remark that simple pyridine rotation process cannot justify the nonrigidity of the CH_2 protons of the {Pd(dppp)} moieties, however, a triflate and/or solvent-assisted decoordination/rotation/coordination equilibria of the {Pd(η^3-2-Me-C_3H_4)(4-PPh_2py)$_2$} units can easily explain the observed facts. The associatively activated substitution of these units for solvent molecules and/or triflate counterions enables its reassembly in an upside down mode, thus providing the mobility of both the pyridine and the {Pd(dppp)} moieties of the system. Mass spectrometry evidences the relative weakness of the M–N_{py} bond (M = Pd or Pt) showing very intense signals of the $[M(\eta^3\text{-2-Me-}C_3H_4)(4\text{-}PPh_2py)_2]^+$ fragments for both compounds **1** and **2** (Supporting Information, Figures S3 and S6). These results are in good agreement with findings reported very recently,[42] and support the theory that the reversible cleavage of M–N_{py} bonds is responsible for the free pyridine rotation, demonstrating that the interchange of the supramolecular species with their components is inherent in the nature of self-assembled systems formed under thermodynamic control.

In summary, we have proved that an adequate choice of building blocks based on their electronic characteristics can induce the self-assembly of a single species, even though the formation of several isomers is possible. The synthesized macrocycles were shown to be stereochemically nonrigid and have offered us a unique opportunity to examine the internal mobility of species self-assembled through metal-coordination chemistry. The metallamacrocycles reported here incorporate, for the first time, allyl-containing corners that can promote catalytic activity in these supramolecules. Work is ongoing to widen the scope of the assembly method using specifically designed building blocks to be explored in catalytic processes.

Acknowledgements

We thank the Ministerio de Ciencia e Innovación (projects: CTQ2009-08795/BQU and CTQ2009-14443-C02-02) and the Deutsche Forschungsgemeinschaft (SFB 624) for financial support.

Keywords: allyl ligands · dynamic behavior · macrocycles · reaction mechanisms · self-assembly

[1] M. Fujita, K. Ogura, *Coord. Chem. Rev.* **1996**, *148*, 249–264.
[2] C. J. Jones, *Chem. Soc. Rev.* **1998**, *27*, 289–299.
[3] P. J. Stang, *Chem. Eur. J.* **1998**, *4*, 19–27.
[4] M. Fujita, *Chem. Soc. Rev.* **1998**, *27*, 417–425.
[5] S. Leininger, B. Olenyuk, P. J. Stang, *Chem. Rev.* **2000**, *100*, 853–907.
[6] G. F. Swiegers, T. J. Malefetse, *Chem. Rev.* **2000**, *100*, 3483–3537.
[7] B. J. Holliday, C. A. Mirkin, *Angew. Chem.* **2001**, *113*, 2076–2097; *Angew. Chem. Int. Ed.* **2001**, *40*, 2022–2043.
[8] F. A. Cotton, C. Lin, C. A. Murillo, *Acc. Chem. Res.* **2001**, *34*, 759–771.
[9] L. Cronin, *Annu. Rep. Prog. Chem. Sect. A: Inorg. Chem.* **2004**, *100*, 323–383.
[10] M. Albrecht, *Naturwissenschaften* **2007**, *94*, 951–966.
[11] K. Ariga, J. P. Hill, M. V. Lee, A. Vinu, R. Charvet, S. Acharya, *Sci. Technol. Adv. Mater.* **2008**, *9*, 014109.
[12] E. Zangrando, M. Casanova, E. Alessio, *Chem. Rev.* **2008**, *108*, 4979–5013.
[13] F. Würthner, C. C. You, C. R. Saha-Moller, *Chem. Soc. Rev.* **2004**, *33*, 133–146.
[14] S. J. Lee, J. T. Hupp, *Coord. Chem. Rev.* **2006**, *250*, 1710–1723.
[15] P. Thanasekaran, R. T. Liao, Y. H. Liu, T. Rajendran, S. Rajagopal, K. L. Lu, *Coord. Chem. Rev.* **2005**, *249*, 1085–1110.
[16] C. L. Chen, J. Y. Zhang, C. Y. Su, *Eur. J. Inorg. Chem.* **2007**, 2997–3010.
[17] N. Gimeno, R. Vilar, *Coord. Chem. Rev.* **2006**, *250*, 3161–3189.
[18] B. H. Northrop, D. Chercka, P. J. Stang, *Tetrahedron* **2008**, *64*, 11495–11503.
[19] M. Ferrer, M. Mounir, O. Rossell, E. Ruiz, M. A. Maestro, *Inorg. Chem.* **2003**, *42*, 5890–5899.
[20] C. C. You, C. Hippius, M. Grune, F. Wurthner, *Chem. Eur. J.* **2006**, *12*, 7510–7519.
[21] A. Sautter, B. K. Kaletas, D. G. Schmid, R. Dobrawa, M. Zimine, G. Jung, I. H. M. van Stokkum, L. De Cola, R. M. Williams, F. Wurthner, *J. Am. Chem. Soc.* **2005**, *127*, 6719–6729.
[22] M. Ferrer, A. Gutierrez, M. Mounir, O. Rossell, E. Ruiz, A. Rang, M. Engeser, *Inorg. Chem.* **2007**, *46*, 3395–3406.
[23] E. Holló-Sitkei, G. Tarkanyi, L. Parkanyi, T. Megyes, G. Besenyei, *Eur. J. Inorg. Chem.* **2008**, 1573–1583.
[24] A. Rang, M. Engeser, N. M. Maier, M. Nieger, W. Lindner, C. A. Schalley, *Chem. Eur. J.* **2008**, *14*, 3855–3859.
[25] A. Rang, M. Nieger, M. Engeser, A. Lutzen, C. A. Schalley, *Chem. Commun.* **2008**, 4789–4791.
[26] P. J. Stang, N. E. Persky, *Chem. Commun.* **1997**, 77–78.
[27] P. Teo, D. M. J. Foo, L. L. Koh, T. S. A. Hor, *Dalton Trans.* **2004**, 3389–3395.
[28] M. C. Álvarez-Vergara, M. A. Casado, M. L. Martin, F. J. Lahoz, L. A. Oro, J. J. Perez-Torrente, *Organometallics* **2005**, *24*, 5929–5936.
[29] K. W. Chi, C. Addicott, M. E. Moon, H. J. Lee, S. C. Yoon, P. J. Stang, *J. Org. Chem.* **2006**, *71*, 6662–6665.
[30] S. Ghosh, D. R. Turner, S. R. Batten, P. S. Mukherjee, *Dalton Trans.* **2007**, 1869–1871.
[31] A. K. Bar, R. Chakrabarty, K. W. Chi, S. R. Batten, P. S. Mukherjee, *Dalton Trans.* **2009**, 3222–3229.
[32] S. Ghosh, P. S. Mukherjee, *Inorg. Chem.* **2009**, *48*, 2605–2613.
[33] Y. F. Han, Y. J. Lin, W. G. Jia, G. X. Jin, *Dalton Trans.* **2009**, 2077–2080.

[34] V. F. Slagt, P. C. J. Kamer, P. W. N. M. van Leeuwen, J. N. H. Reek, *J. Am. Chem. Soc.* **2004**, *126*, 1526–1536.
[35] I. Angurell, O. Rossell, M. Seco, E. Ruiz, *Organometallics* **2005**, *24*, 6365–6373.
[36] R. G. Pearson, *Inorg. Chem.* **1973**, *12*, 712–713.
[37] X-ray diffraction data: $3C_4H_{10}O$, $18CF_3O_3S$, $6CH_2Cl_2$, $8H_2O$: $3C_{130}H_{122}N_4P_8Pd_2Pt_2$, $M_w = 11316.35$, $T = 100(2)$ K, $Mo_{K\alpha}$ radiation (0.71073 Å), triclinic, $P\bar{1}$, $a = 14.1390(6)$ Å, $b = 32.3082(15)$ Å, $c = 52.607(3)$ Å, $\alpha = 94.867(5)°$, $\beta = 90.932(3)°$, $\gamma = 93.912(3)°$, $V = 23882.8(19)$ Å^3, $Z = 2$, $\rho_{calcd} = 1.574$ g cm^{-3}, $\mu = 2.284$ mm^{-1}, $F(000) = 11300$, crystal size $0.33 \times 0.23 \times 0.02$ mm^3, $1.29° \leq \theta \leq 25.68°$, measured reflections 338227, independent reflections 90632 [$R_{int} = 0.0984$], max. and min. transmission: 0.5598 and 0.5598, data/restraints/parameters 90632/7155/5620, $R1 = 0.0781$, $wR2 = 0.1719$ [$I > 2\sigma$], $R1 = 0.1388$, $wR2 = 0.2034$ [all data], GOF = 1.093, largest diff. peak and hole 3.501 and −2.032 e Å^{-3}. CCDC-784032 contains the supplementary crystallographic data for this paper. These data can be obtained free of charge from The Cambridge Crystallographic Data Centre via www.ccdc.cam.ac.uk/data_request/cif.
[38] Z. Q. Qin, M. C. Jennings, R. J. Puddephatt, *Chem. Commun.* **2001**, 2676–2677.
[39] D. E. Janzen, K. N. Patel, D. G. VanDerveer, G. J. Grant, *Chem. Commun.* **2006**, 3540–3542.
[40] M. Capo, J. Benet-Buchholz, P. Ballester, *Inorg. Chem.* **2008**, *47*, 10190–10192.
[41] D. C. Caskey, T. Yamamoto, C. Addicott, R. K. Shoemaker, J. Vacek, A. M. Hawkridge, D. C. Muddiman, G. S. Kottas, J. Michl, P. J. Stang, *J. Am. Chem. Soc.* **2008**, *130*, 7620–7628.
[42] J. Vacek, D. C. Caskey, D. Horinek, R. K. Shoemaker, P. J. Stang, J. Michl, *J. Am. Chem. Soc.* **2008**, *130*, 7629–7638.
[43] G. Tárkányi, H. Jude, G. Palinkas, P. J. Stang, *Org. Lett.* **2005**, *7*, 4971–4973.
[44] P. V. Bernhardt, C. Gallego, M. Martinez, T. Parella, *Inorg. Chem.* **2002**, *41*, 1747–1754.
[45] M. Font-Bardía, C. Gallego, G. Gonzalez, M. Martinez, A. E. Merbach, X. Solans, *Dalton Trans.* **2003**, 1106–1113.
[46] A. Pastor, E. Martinez-Viviente, *Coord. Chem. Rev.* **2008**, *252*, 2314–2345.
[47] M. L. Tobe, J. Burgess, *Inorganic Reaction Mechanisms*, Longman, Essex, **1999**.

Received: September 9, 2010
Published online: November 12, 2010

